Influence of association on the liquid–vapor phase coexistence of simple systems

Fernando Bresme
Departamento de Química-Física, Facultad de CC. Químicas, Universidad Complutense de Madrid, E-28040, Spain and Instituto de Química-Física Rocasolano, CSIC, Serrano 119, E-28006 Madrid, Spain

Enrique Lomb
Instituto de Química-Física Rocasolano, CSIC, Serrano 119, E-28006 Madrid, Spain

José L. F. Abascal
Departamento de Química-Física, Facultad de CC. Químicas, Universidad Complutense de Madrid, E-28040, Spain

(Received 17 September 1996; accepted 15 October 1996)

The liquid–vapor phase diagram of an associating fluid interacting via a central force model potential is computed by means of the Gibbs ensemble Monte Carlo simulations. The Hamiltonian contains two components, a harmonic oscillator potential which allows for chemical association of particles and a Lennard-Jones interaction. The bonding potential depends on three parameters, bonding distance L, potential depth D_e, and force constant k_e. We have studied the influence of L on the phase coexistence properties of the system. For small L the liquid phase shrinks and the results suggest that for short enough L, the stable liquid phase disappears. In addition to this, the coexistence curves exhibit a large change in the coexistence densities as bonding distance is shortened. The fitting of the coexistence data to scaling laws shows that a classical value for the critical exponent β may be adequate to describe the phase boundaries of a system with short bonding distance whereas both classical and Ising values would be suitable to describe the coexistence densities for a large L. Finally, the effect of association on the asymmetry of the liquid–vapor coexistence curve is discussed. © *1997 American Institute of Physics.* [S0021-9606(97)50304-7]

I. INTRODUCTION

Liquid–vapor coexistence of simple fluids has been the focus of a number of works for quite some time. From systematic studies with simple potentials such as Yukawa, Stockmayer, or Lennard-Jones, it is known that for a short enough interaction potential range,[1–5] the fluid only undergoes a direct phase transition to the solid. This feature has been observed experimentally[6,7] in the context of colloidal science and theoretical studies have further confirmed it.[8,9] The investigation of the conditions for the appearance or not of a liquid-vapor transition can be made through the use of computer simulations. In this context, the Gibbs ensemble technique[10] has contributed to a great extent in the last years (see Ref. 11 for a review). The computation of the coexistence region has also been extended to the field of associating fluids. These are characterized by a Hamiltonian which allows for association of particles to form molecules. The topology and number of the so-formed molecules depends on the peculiarities of the Hamiltonian. As discussed by Kalyuzhnyi *et al.*[12] the associating fluids can be modeled either by means of potential in which association is due to off-center sites, or through center–center type associating potentials (central force models). In addition, there might be mixed potentials which share peculiarities from both models. Several studies on the first class of potentials can be found in the literature.[13–17] It is to be recalled here that the celebrated Wertheim's[18] theory for associating fluids reproduces to a great extent the thermodynamics and association of these systems.

The phase stability of these models has been considered as well. The coexistence curves are similar to that of simple fluids, and an Ising value for the critical exponent β gives good account of the shape of the phase coexistence boundaries.[15] As mentioned previously, the use of central force potentials is a sensible alternative to the study of associating fluids. This is the type of systems that Cummings and Stell[19,20] considered in their pioneering work on association reactions.

Recently, we reported theoretical and simulation results for a central force model fluid of the type mentioned above.[21] A preliminary study of the phase stability of the system showed that variations in the bonding distance, L, result in dramatic changes of the phase behavior. It was observed that the stability of the liquid phase could be inhibited for short enough values of L, and that an intermediate regime between this and a Lennard-Jones fluid behavior would appear for larger values of L. These conclusions, however, were based in results obtained from the analysis of the pseudospinodal line of the HNC integral equation. Therefore, in order to extent and complement those results, in this work we report on the coexistence properties of the aforementioned model, and their dependence on L as obtained from Gibbs ensemble Monte Carlo simulations. The present results confirm our previous preliminary conclusions based on the HNC integral

equation. We will see that the crucial changes in the shape of the phase diagrams do actually defy the law of corresponding states and are closely connected with the chemical nature of the system, an interesting feature observed experimentally in apparently unrelated systems such as electrolytes[22] and, very especially, liquid metals.[23]

II. POTENTIAL MODEL AND GIBBS ENSEMBLE SIMULATIONS

The potential model was described in full detail in Ref. 21, so we only include here a brief recollection of its main features for the sake of completeness. Particles are allowed to associate by the introduction of a bonding potential, U_{bond}. In addition, particles interact through a Lennard-Jones potential, U_{LJ}. The expression for each contribution can be written as follows:

$$U_{\mathrm{bond}}(r)=\tfrac{1}{2}k_e(r-L)^2+D_e, \tag{2.1}$$

$$U_{\mathrm{LJ}}(r)=4\epsilon\left[\left(\frac{\sigma}{r}\right)^{12}-\left(\frac{\sigma}{r}\right)^{6}\right]. \tag{2.2}$$

L sets the bond length, D_e defines the depth, and k_e is the force constant of the bonding potential. As usually, ϵ represents the Lennard-Jones potential depth and σ the particle diameter. These parameters ϵ and σ are used throughout this work to define reduced quantities. Thus we have the reduced density $\rho^*=N\sigma^3/V$ (N being the total number of particles filling a volume V), temperature $T^*=k_BT/\epsilon$, pressure $P^*=P\sigma^3/\epsilon$, and chemical potential $\mu^*=\mu/\epsilon$. Similarly, we define for the bonding potential the reduced bonding distance $L^*=L/\sigma$, and force constant $k_e^*=k_e\sigma^2/\epsilon$.

Once both bonding and LJ contributions have been given one can write the total potential,

$$U_{\mathrm{TOT}}(r)=U_{\mathrm{bond}}(r)[1-l(r)]+U_{\mathrm{LJ}}(r)l(r) \tag{2.3}$$

being $l(r)$ a function which has the effect of switching between the bonding and the Lennard-Jones contribution along the distance. As in our previous work, $l(r)$ is defined as

$$l(r)=\frac{1}{2}\left[1+\tanh\left(\frac{r-R}{w}\right)\right]. \tag{2.4}$$

In the current application, the potential depth D_e of the bonding contribution (2.1) is set to zero, $R=0.78$ and $w=0.012$ and the force constant $k_e^*=15\,000$. As discussed in Ref. 21, the value for D_e has an important effect on the phase coexistence curve. The choice made here for D_e leads to a considerably polydisperse system. Another important consideration about the model potential used in this work is that, for $L^*<0.5$, the possibility to form clusters of different sizes and shapes is greatly reduced by simple geometric considerations. The possible clusters for these short bonding distances involve few particles, the largest being four-particle clusters. For larger bonding distances, the clusters observed are more linear and it exists the possibility of bifurcated bonds. This effect is particularly noticeable at high densities where association is enhanced.

The liquid–vapor equilibria of a system of particles interacting through the potential (2.3) was computed by means of Gibbs ensemble Monte Carlo (GEMC) simulation. This technique has been described extensively in several reviews, so we refer the reader to these works for a detailed discussion.[10,11] Some considerations have to be made when simulating associating fluids. As pointed out in our previous paper[21] the particles have to be able to get in and out of the range of the bonding potential. This is accomplished by considering two types of particle displacements. The associated maximum displacements are randomly chosen in each MC step with equal probabilities. In this way we will generate movements in intermolecular and intramolecular scales. In the intramolecular scale we have chosen a maximum displacement $\delta r=0.15\sigma$ and for intermolecular ranges we have considered $\delta r\approx 0.5-0.75\sigma$. For low densities ($\rho^*\leqslant 0.2$), δr was set to half the box length and this was used as the unique displacement value for the particles. The cutoff of the potential energy was set at half the box length.

The GEMC simulations were divided in cycles, each composed of N trial displacements, N_i interchanges, and 1 change in volume. The systems studied are modeled with either $N=300$ or $N=500$ particle samples. The acceptance rate of particle exchanges was 0.5%–3% and the maximum volume change was tuned to lead to an acceptance ratio of 50%. The equilibration period typically needed between 5000 and 10 000 cycles and the production run was extended during 10 000–15 000 additional cycles. Block subaverages were used to compute averages of the desired quantities as well as their corresponding standard deviations.

TABLE I. Simulation results for $L^*=0.45$. Numbers in parenthesis represent the error of the data taken as one standard deviation of the mean. Number of particles was $N=500$ for all data.

T^*	ρ_v^*	ρ_l^*	U_v^*	U_l^*	P_v^*	P_l^*	μ_v^*	μ_l^*
1.20	0.135 (8)	1.387 (17)	−1.09 (8)	−8.71 (11)	0.088 (8)	0.085	−3.50	−3.98
1.21	0.140 (8)	1.341 (19)	−1.13 (8)	−8.42 (11)	0.091 (8)	0.070	−3.52	−3.58
1.22	0.155 (14)	1.290 (25)	−1.25 (12)	−8.13 (14)	0.094 (10)	0.110	−3.52	−3.57
1.24	0.172 (11)	1.183 (22)	−1.36 (9)	−7.52 (13)	0.099 (11)	0.110	−3.52	−3.66
1.25	0.191 (16)	1.148 (39)	−1.52 (14)	−7.34 (23)	0.099 (14)	0.074	−3.55	−3.46
1.27	0.224 (16)	1.094 (30)	−1.71 (14)	−6.99 (18)	0.106 (18)	0.110	−3.56	−3.62
1.30	0.239 (24)	0.986 (19)	−1.81 (19)	−6.34 (11)	0.115 (25)	0.121	−3.56	−3.51
1.31	0.263 (25)	0.905 (52)	−1.95 (17)	−5.86 (31)	0.117 (20)	0.108	−3.58	−3.54

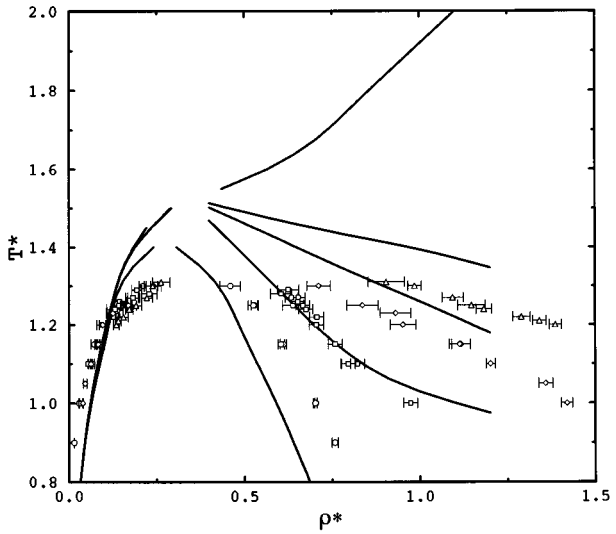

FIG. 1. Liquid–vapor diagram for the potential (2.3) as a function of the bonding distance L^*. Circles represents the Lennard-Jones system, squares are for $L^*=0.7$, diamonds $L^*=0.5$, and triangles $L^*=0.45$. Lines are the pseudospinodal for these systems as predicted by the HNC integral equation for the LJ system, $L^*=0.7$, $L^*=0.5$, $L^*=0.45$, and $L^*=1/3$.

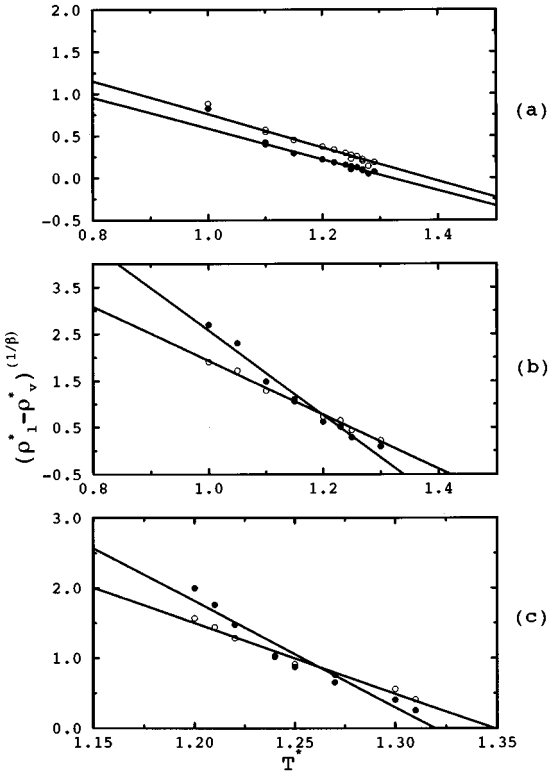

FIG. 2. Fitting of GEMC simulation data to the scaling law given by Eq. (3.3) for three bonding distances (a) $L^*=0.7$, (b) $L^*=0.5$, and (c) $L^*=0.45$. White circles are for $\beta=0.5$ and black circles for $\beta=0.325$.

III. RESULTS

A. Liquid–vapor coexistence

The liquid–vapor equilibrium of the system described by the potential (2.3) is presented in Fig. 1 for three bonding distances $L^*=0.45$, 0.5, and 0.70. Numerical results are compiled in Tables I–III. In Fig. 1 we have included for comparison results for the Lennard-Jones potential (data taken from Ref. 24). The Gibbs ensemble results confirm our previous impressions based on the HNC integral equation. Shortening the bonding distance results in a shrinking of the stability region of the liquid phase. It appears that the HNC pseudospinodal curve represents a good approximation to the liquid branch for the system at $L^*=0.7$. Nevertheless, this fact must be interpreted more as a coincidence than as a virtue of the theory. Indeed we observe that the pseudospinodal curve lies outside the liquid branch for $L^*=0.45$, and 0.5, whereas it is inside the liquid branch for the Lennard-Jones potential. Nevertheless, the HNC pseudospinodal curve gives qualitatively all the trends of the liquid–vapor equilibria including features such as the change in the slope of the liquid coexistence line for $L^*=0.7$ at temperatures lower than $T^*=1.1$.

We have not attempted to compute the coexistence for the bonding distance $L^*=1/3$ because the Gibbs ensemble results together with the HNC predictions suggest that a decrease in the bonding distance would eventually lead to the disappearance of the liquid phase. Thus the phase diagram would reduce to a fluid–solid equilibrium. This feature has been reported by different authors in the study of Yukawa systems,[4,5] although in the latter instance the liquid phase becomes unstable when shrinking the range of the potential. We recover here the same observation by varying the bonding distance.

TABLE II. Simulation results for $L^*=0.5$. Number of particles $N=500$ for all data.

T^*	ρ_v^*	ρ_l^*	U_v^*	U_l^*	P_v^*	P_l^*	μ_v^*	μ_l^*
1.00	0.0395 (14)	1.420 (16)	−0.368 (19)	−8.77 (8)	0.0314 (11)	0.044	−3.64	−4.04
1.05	0.0464 (53)	1.359 (20)	−0.412 (51)	−8.38 (10)	0.0378 (33)	0.038	−3.68	−3.95
1.10	0.0630 (28)	1.202 (13)	−0.558 (31)	−7.56 (9)	0.0500 (24)	0.059	−3.64	−3.51
1.15	0.0828 (40)	1.118 (27)	−0.711 (38)	−7.09 (16)	0.0643 (31)	0.073	−3.62	−3.48
1.15	0.0831 (47)	1.114 (30)	−0.715 (47)	−7.06 (17)	0.0640 (30)	0.071	−3.62	−3.52
1.20	0.0957 (90)	0.953 (37)	−0.799 (81)	−6.13 (21)	0.0752 (45)	0.077	−3.66	−3.76
1.23	0.125 (19)	0.932 (43)	−1.01 (15)	−5.98 (25)	0.0893 (74)	0.089	−3.59	−3.69
1.25	0.170 (22)	0.838 (45)	−1.36 (16)	−5.44 (26)	0.1019 (84)	0.091	−3.57	−3.57
1.30	0.242 (10)	0.712 (33)	−1.826 (97)	−4.67 (20)	0.117 (20)	0.100	−3.59	−3.61

TABLE III. Simulation results for $L^*=0.7$.

T^*	ρ_v^*	ρ_l^*	U_v^*	U_l^*	P_v^*	P_l^*	μ_v^*	μ_l^*
1.00[a]	0.035 (6)	0.974 (20)	−0.314 (64)	−6.20 (11)	0.029 (4)	0.057	−3.71	−3.66
1.10[a]	0.0548 (8)	0.796 (20)	−0.457 (71)	−5.20 (12)	0.046 (5)	0.049	−3.71	−3.72
1.10[b]	0.0671 (50)	0.823 (20)	−0.592 (50)	−5.34 (11)	0.050 (52)	0.059	−3.62	−3.72
1.15[a]	0.087 (14)	0.759 (20)	−0.72 (12)	−4.95 (11)	0.065 (7)	0.061	−3.59	−3.65
1.20[b]	0.094 (14)	0.705 (20)	−0.79 (12)	−4.63 (13)	0.073 (7)	0.063	−3.67	−3.66
1.22[b]	0.129 (12)	0.706 (20)	−1.05 (10)	−4.61 (14)	0.088 (8)	0.079	−3.59	−3.58
1.24[b]	0.131 (23)	0.675 (20)	−1.03 (18)	−4.42 (12)	0.091 (11)	0.082	−3.60	−3.58
1.25[a]	0.164 (17)	0.639 (30)	−1.27 (14)	−4.20 (20)	0.103 (10)	0.091	−3.55	−3.58
1.25[b]	0.142 (20)	0.667 (20)	−1.12 (17)	−4.37 (11)	0.096 (11)	0.097	−3.58	−3.61
1.26[b]	0.144 (19)	0.653 (20)	−1.12 (14)	−4.28 (10)	0.101 (12)	0.098	−3.59	−3.58
1.27[a]	0.183 (15)	0.635 (18)	−1.38 (12)	−4.16 (11)	0.108 (22)	0.082	−3.53	−3.55
1.27[b]	0.181 (20)	0.654 (20)	−1.40 (16)	−4.28 (13)	0.104 (17)	0.109	−3.57	−3.58
1.28[a]	0.229 (22)	0.605 (30)	−1.71 (17)	−3.98 (19)	0.105 (34)	0.090	−3.55	−3.52
1.29[b]	0.193 (14)	0.626 (30)	−1.46 (11)	−4.11 (15)	0.113 (20)	0.099	−3.57	−3.58

[a]$N=300$.
[b]$N=500$.

A remarkable feature of systems with bonding distances $L^*=0.45$ and 0.5 is the large asymmetry of the coexistence curve as compared to the system $L^*=0.7$ or the LJ fluid. Since apparently the critical density does not change substantially with the bonding distance, these results resemble in some way the behavior observed in ionic and some metallic systems. We will come back to this point later on.

B. Scaling laws

Once the liquid–vapor coexistence lines are known one can study to what extent the shape of the curves matches the expected theoretical behavior. The critical behavior can be expressed mathematically in terms of power laws whose critical exponents define the universality class to which the system pertains. An usual power law relates the reduced density difference in coexistent phases $\Delta\rho^*=(\rho_l-\rho_v)/\rho_c$ with the reduced temperature distance $\Delta T^*=(T-T_c)/T_c$ as,

$$\Delta\rho^*=C|\Delta T^*|^{\beta}, \tag{3.1}$$

where the l and v in the previous expression refer to liquid and vapor phases, and the subindex c denotes properties at the critical point. The critical exponent β is about 1/3 for the universality class of the three-dimensional Ising model and it has been known for a long time that many simple fluids follow this behavior. Nevertheless, the situation is not so clear when ionic fluids are involved. As compared to simple fluids such as argon, ionic fluids are characterized by a remarkable volume change at coexistence, as noted by Kirshenbaum *et al.*[25] Recent works[26–29] on the critical properties of ionic fluids have exposed the differences between neutral and ionic systems. From a practical standpoint ionic fluids are deemed to have classical exponents. Nevertheless, the situation in the immediate vicinity of the critical point is quite unclear with respect to a possible crossover of the exponent from classical to Ising values. In a recent work by Caillol *et al.*[30] the critical behavior of the restricted primitive model (RPM) of electrolytes has been computed using refined simulation techniques. The authors concluded that the critical behavior might be of the Ising type. The situation remains so far somewhat inconclusive.

If one tries to describe the very vicinity of the critical point, a Wegner expansion[31] of the density should be used in order to fit the coexistence curve. Nevertheless, this region is quite difficult to handle by means of GEMC so one is constrained to apply the analysis to a certain distance from the critical point. Therefore, whereas we will be making use of scaling laws to fit our simulation data, we will not dwell any further on the issue of the ''true'' criticality of the systems considered herein. Far enough from the critical point the Wegner series tends to diverge but it has been observed that a truncation of this series up to the first term is able to reproduce the critical behavior of simple systems in this region. This fact has been confirmed in several studies.[32,33] The equations then reduce to the well known rectilinear diameter law,[34]

$$\frac{\rho_l^*+\rho_v^*}{2}=A+BT^* \tag{3.2}$$

TABLE IV. Constant values for the rectilinear diameter law (3.2) and scaling law (3.3).

	$\beta=1/2$						$\beta=0.325$			
L^*	A	B	C	D	T_c^*	ρ_c^*	C	D	T_c^*	ρ_c^*
LJ	0.512	−0.141					1.264	0.967	1.31	0.33
0.7	0.582	−0.139	2.738	1.979	1.38	0.39	2.423	1.825	1.33	0.40
0.5	1.630	−0.898	7.713	5.781	1.33	0.44	11.628	9.052	1.28	0.48
0.45	2.544	−1.492	13.603	10.086	1.35	0.53	19.995	15.151	1.32	0.57

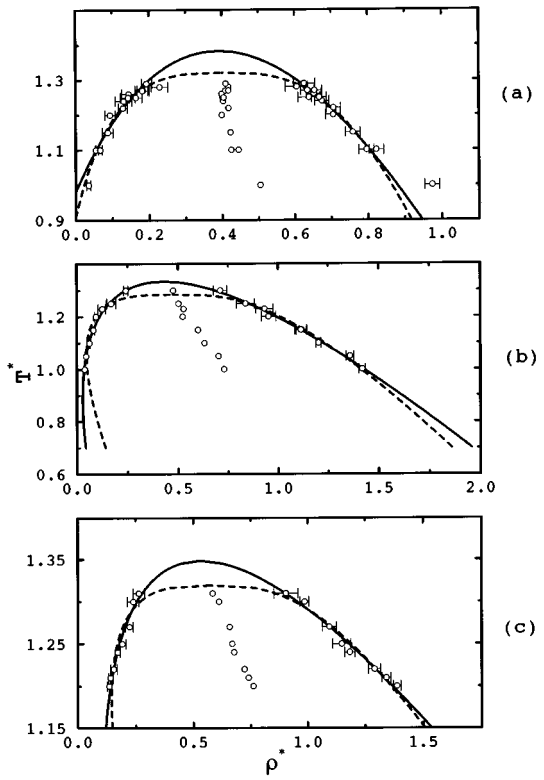

FIG. 3. Comparison of the simulated liquid–vapor equilibria with the phase coexistence boundaries predicted by Eqs. (3.2) and (3.3) and the coefficients of Table IV, as a function of the bonding distance: (a) $L^*=0.7$, (b) $L^*=0.5$, and (c) $L^*=0.45$. Dashed lines are for $\beta=0.325$ and full lines for $\beta=0.5$.

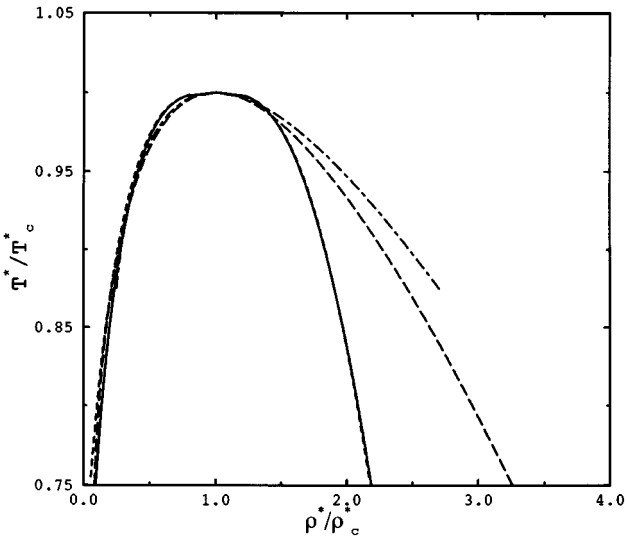

FIG. 4. Reduced temperature T^*/T_c^* as a function of reduced density ρ^*/ρ_c^*. Full lines represent the LJ($\beta=0.325$) system, short-dashed $L^*=0.7(\beta=0.325)$, long-dashed $L^*=0.5(\beta=0.5)$, and dot–dashed $L^*=0.45(\beta=0.5)$.

and the scaling law for density,[35]

$$(\rho_l^*-\rho_v^*)^{1/\beta}=C-DT^*, \tag{3.3}$$

where $T_c^* = C/D$. We have fitted our data to these expressions and estimated the values of the constants, A, B, C, and D for the classical and the Ising values of β. The fittings are shown in Fig. 2 and numerical values for the constants are compiled in Table IV. Figure 2(b) shows that the bonding distance $L^*=0.5$ results fit well to a straight line when the $\beta=0.5$ is considered. The same data adjusted to the scaling law but considering an Ising exponent $\beta=0.325$ deviate from the expected linear behavior. For larger bonding distance, $L^*=0.7$ [cf. Fig. 2(a)] both exponents lead to a linear dependence. Notice that the data at $T^*=1.0$ significantly deviate from the straight line. This is a consequence of the change in the slope of the liquid branch at those temperatures, fact observed both in the simulation and the HNC results (see Fig. 1). The same fitting procedure on the system with the shortest bonding distance, $L^*=0.45$, leads to the results reported in Fig. 2(c). This shows again that a classical exponent is valid for fitting the results for such short bonding distances. Finally, the analysis performed on the Lennard-Jones fluid (not shown) is consistent with a linear dependence when an Ising exponent is used.

In summary, a classical exponent seems adequate to describe the shape of the coexistence curve for short bonding distances in a region not too close to the critical point. For a larger bonding distance $L^*=0.7$ both mean field and Ising exponents would describe correctly the shape of the coexistence curve. Nevertheless, each of the exponents would lead to different critical temperatures and densities, and only an examination of the coexistence curve in the neighborhood of the critical point would allow to determine to which universality class the system pertains. In order to analyze this further, one would be compelled to use refined computational techniques that can cope with finite size effects, as those employed by Caillol *et al.*[30] Therefore, we must insist here that our β exponent should not be thought as indicative of the ''true'' critical exponent of the model.

In Fig. 3 we have depicted the simulation data jointly with the fitted scaled law and the rectilinear diameter law. It is clear that the fitting for $L^*=0.45$ and $L^*=0.5$ using the classical exponent for β reproduces the shape of the curve. Note that the use of an Ising exponent would lead to a too low critical temperature, not confirmed by the GEMC results. With respect to $L^*=0.7$ it is not clear which exponent would hold in the vicinity of the critical point, given the difficulty to obtain reliable simulation data in this region. Nevertheless, it is interesting to note the coincidence of the fit obtained from both exponent values at temperatures far enough from the critical point. Again, it is to be pointed out the large deviation of the liquid coexistence density at temperature $T^*=1.0$ from the scaling law prediction. This fact was already noted and justified when discussing Fig. 2(a).

Table IV collects the critical densities and temperatures extracted from Eqs. (3.2) and (3.3). We see that use of Ising exponents tends to give lower critical temperatures and larger critical densities than classical exponents. A shortening of the bonding distance turns out in higher critical densities. This observation is independent on the exponent used. Since the change in the bonding distance is the source of a large change in the associating character of the systems,[21] the

general trends obtained from the data of Table IV can be taken as indicative of the effect that association has on the critical properties of these fluid models.

Once the critical values of temperature and density are known, following Kirshenbaum *et al.*,[25] it is worthwhile to replot the coexistence curves as a function of these constants. We have used an Ising exponent for the LJ and $L^*=0.7$ systems and the classical value for the two remaining bonding distances. Short bonding distances $L^*=0.45$, 0.5 present a large density rate expansion (cf. Fig. 4), as observed in ionic liquids. For larger bonding distances the system closely resembles the LJ model, which is a valid representation of a typical atomic fluid such as argon. It is important to stress that a different choice for the critical exponents would slightly reshape the curves but does not affect the above conclusions.

This violation of the corresponding states law is a well known phenomenon in liquid metals.[23] In that case, it is a result of the different nature of the net interparticle interaction in the gas and the liquid phases. Hensel has shown that dimerization in the gaseous Cs and Rb leads to quite asymmetric coexistence curves, similar to those obtained in this work for short bonding distances (see Fig. 4). For Hg, for which clustering in the gas phase is less important, the curve is much more symmetric. In our case we observe similar behavior but the explanation seems to be somewhat different. At low densities, irrespective of the bonding distance, our systems do not exhibit a great tendency to associate, thus they can be viewed as atomic fluids (see Table III of Ref. 21). By contrast, it is in the liquid phase where the systems show a significant associative behavior. Irrespective of the phase where the main changes in association take place, one must expect a unique response of the system to these features, which seems to translate into an asymmetry of the coexistence curve. A tentative conclusion then may be that the phase diagram asymmetry can be correlated to particle association, being irrelevant in which phase the latter takes place.

IV. SUMMARY AND DISCUSSION

The liquid–vapor phase diagram of an associating potential model has been studied by means of GEMC simulations. The Hamiltonian is of the central force model type and is composed of two parts, and harmonic oscillator like potential, which allows for association between particles at distances shorter than the particle diameter σ, and a second contribution modeled as a Lennard-Jones potential. The associating potential involves three parameters, bonding distance L, potential depth D_e, and force constant k_e. In this work we have analyzed the influence of varying L, at constant D_e and k_e, over the phase coexistence boundaries. Our choice of $D_e=0$ implies that the system present a large degree of polydispersity, as discussed in Ref. 21. The GEMC computations confirm our previous conclusions based on the analysis of the HNC pseudospinodal line for this Hamiltonian. For short bonding distances, the stability region of the liquid phase shrinks. Although we have not attempted to compute the fluid–solid equilibria for this system, the HNC results together with the simulation data seem to indicate the disappearance of the liquid phase for short enough bonding distances and the reduction of the phase diagram to a fluid–solid equilibrium. Similar effects have been reported as a consequence of changes in the range of the potential.[4,5] However, in that case, this effect is not accompanied by a large increase in the coexistence liquid density with temperature as it has been observed in the present instance.

Recent works on the phase equilibria of dipolar hard spheres seem to confirm that this system has not a stable liquid phase.[1,2] An explanation to this observation has been given[36,37] based on the formation of chains which interact weakly. Under such circumstances the system is unable to render a stable liquid phase. Following the same line of reasoning we can try to explain the features observed in this work. From the cluster analysis made in our preceding paper[21] we know that for $L^*<0.5$ the ability to form clusters of different sizes and shapes is greatly reduced by simple geometric considerations. In such a case, the clusters are very compact and involve few particles (four at most). In comparison larger bonding distances render clusters more linear and it exists the possibility of bifurcated bonds. This effect is specially noticeable at high densities where association is enhanced. It is then expected that, at short bonding distances, the excluded volume entropy is not counterbalanced by the energetic contribution to the extent that the liquid phase is no longer stable. It is tempting to relate the origin of the peculiar behavior of ionic systems and fluid metals to the ideas exposed above.

We have fitted the phase coexisting data to a scaling law by assuming either classical or Ising values for the critical exponent β. It is important to note here that these results are relevant only for a range of temperatures which are rather far from the critical one, hence our results do not aim to represent real exponents. It is, however, remarkable the differences exhibited by our fitted critical exponents at different values of L. We have found that a classical exponent seems to be valid for bonding distances $L^*=0.45$, 0.5, whereas the situation is unclear at larger values, like $L^*=0.7$. In the latter case both exponents give good account of the shape of the curve. From the scaling laws we have estimated the critical parameters of the model as a function of bonding distance. Irrespective of the exponent considered, the critical density increases as L^* is shortened. As this has the effect of reducing the chain length of the clusters formed, this result is in agreement with previous works[14] dealing with the phase equilibria of associating chains.

ACKNOWLEDGMENT

This work was partially supported by Grants No. PB93-0085 and No. PB94-0112 furnished by the Dirección General de Investigación Científica y Tecnológica of Spain.

[1] M. E. van Leeuwen and B. Smit, Phys. Rev. Lett. **71**, 3991 (1993).
[2] J. J. Weis and D. Levesque, Phys. Rev. Lett. **71**, 2729 (1993).

[3] M. H. J. Hagen, E. J. Meijer, G. C. A. M. Mooij, D. Frenkel, and H. N. W. Lekkerkerker, Nature (London) **365**, 425 (1993).
[4] E. Lomba and N. G. Almarza, J. Chem. Phys. **100**, 8367 (1994).
[5] M. H. J. Hagen and D. Frenkel, J. Chem. Phys. **101**, 4093 (1994).
[6] F. Leal Calderon, J. Bibette, and J. Biais, Europhys. Lett. **23**, 653 (1993).
[7] P. N. Pusey, W. C. K. Poon, S. M. Ilett, and P. Barlett, J. Phys. **6**, A29 (1994).
[8] A. P. Gast, C. K. Hall, and W. B. Russell, J. Colloid Interface Sci. **96**, 251 (1983).
[9] H. N. W. Lekkerkerker, W. C. K. Poon, P. N. Pusey, A. Stroobants, and P. B. Warren, Europhys. Lett. **20**, 559 (1992).
[10] A. Z. Panagiotopoulos, Mol. Phys. **61**, 813 (1987).
[11] A. Z. Panagiotopulos, in *Observation, Prediction and Simulation of Phase Transitions in Complex Fluids*, edited by M. Baus, L. F. Rull, and J. P. Ryckaert NATO ASI Series Vol. 460 (1995), and references therein.
[12] Y. V. Kalyuzhnyi, G. Stell, M. L. Llano-Restrepo, W. G. Chapman, and M. F. Holovko, J. Chem. Phys. **101**, 7939 (1994).
[13] G. Jackson, W. G. Chapman, and K. E. Gubbins, Mol. Phys. **65**, 1 (1988).
[14] W. G. Chapman, G. Jackson, and K. E. Gubbins, Mol. Phys. **65**, 1057 (1988).
[15] J. K. Johnson and K. E. Gubbins, Mol. Phys. **77**, 1033 (1992).
[16] J. M. Walsh and K. E. Gubbins, Mol. Phys. **80**, 65 (1993).
[17] R. P. Sear and G. Jackson, J. Chem. Phys. **102**, 939 (1995).
[18] M. S. Wertheim, J. Stat. Phys. **35**, 19 (1984); *ibid*. **35**, 35.
[19] P. T. Cummings and G. Stell, Mol. Phys. **51**, 253 (1984).
[20] P. T. Cummings and G. Stell, Mol. Phys. **55**, 33 (1988).
[21] F. Bresme, J. L. F. Abascal, and E. Lomba, J. Chem. Phys. **105**, 10008 (1996).
[22] H. Gasbrenner and H. Weingärtner, J. Phys. Chem. **93**, 3378 (1989).
[23] F. Hensel, J. Phys. Condensed Matter **2**, SA33 (1990).
[24] A. Z. Panagiotopoulos, N. Quirke, M. Stapleton, and D. J. Tildesley, Mol. Phys. **63**, 527 (1988).
[25] A. D. Kirshenbaum, J. A. Cahill, P. J. McGonigal, and A. V. J. Grosse, J. Inorg. Nucl. Chem. **24**, 1287 (1962).
[26] J. M. H. Levelt Sengers, and J. A. Given, Mol. Phys. **80**, 899 (1993).
[27] M. E. Fisher, J. Stat. Phys. **75**, 1 (1994).
[28] G. Stell, J. Stat. Phys. **78**, 197 (1995).
[29] K. S. Pitzer, J. Phys. Chem. **99**, 13070 (1995).
[30] J. M. Caillol, D. Levesque, and J. J. Weis, Phys. Rev. Lett. **77**, 2039 (1996).
[31] F. Wegner, Phys. Rev. B **5**, 4529 (1972).
[32] L. Vega, E. de Miguel, L. F. Rull, G. Jackson, and I. A. McLure, J. Chem. Phys. **96**, 2296 (1992).
[33] D. Green, G. Jackson, E. de Miguel, and L. F. Rull, J. Chem. Phys. **101**, 3190 (1994).
[34] J. S. Rowlinson and F. L. Swinton, *Liquids and Liquid Mixtures*, 3rd ed. (Butterworths, London, 1982).
[35] J. S. Rowlinson and B. Widom, *Molecular Theory of Capillarity* (Clarendon, Oxford, 1982).
[36] R. P. Sear, Phys. Rev. Lett. **76**, 2310 (1996).
[37] R. van Roij, Phys. Rev. Lett. **76**, 3348 (1996).